

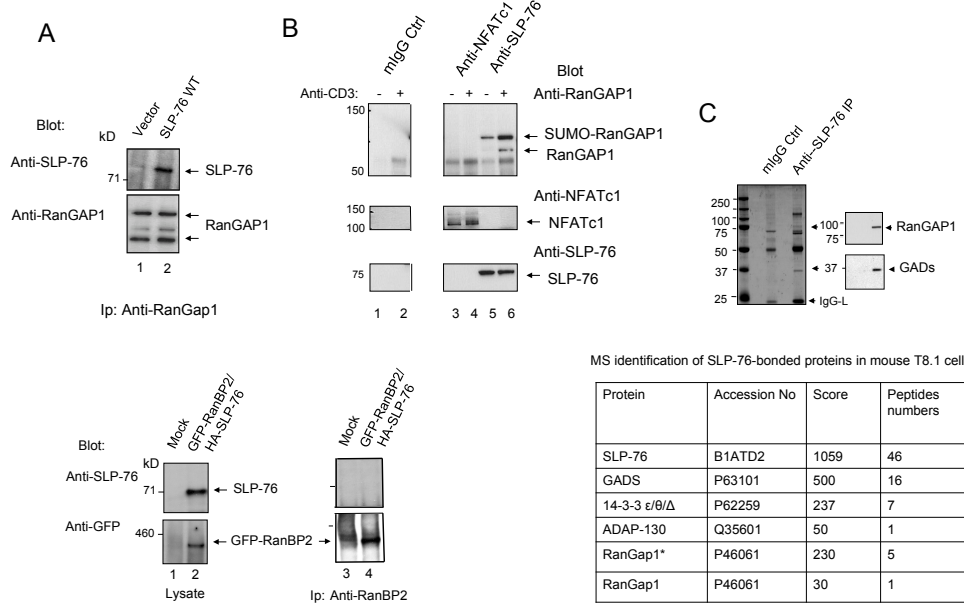
Molecular Cell, Volume 59

Supplemental Information

The Immune Adaptor SLP-76 Binds to SUMO-RANGAP1 at Nuclear Pore Complex Filaments to Regulate Nuclear Import of Transcription Factors in T Cells

Hebin Liu, Helga Schneider, Asha Recino, Christine Richardson, Martin W. Goldberg,
and Christopher E. Rudd

Figure S1



(C) (continued)

[tr|Q6NZB5|Q6NZB5_MOUSE](#) Mass: 64005 Score: 230 Matches: 5(4) Sequences: 5(4) emPAI: 0.28
Rangap1 protein OS=Mus musculus GN=Rangap1
 Check to include this hit in error tolerant search or archive report

Query	Observed	Mr(expt)	Mr(calc)	ppm	Miss	Score	Expect	Rank	Unique	Peptide
✓ 566	496.7580	991.5014	991.5008	0.63	0	33	0.012	1	U	K.GGVNARETLK.T + Oxidation (M)
✓ 1076	568.3101	1134.6057	1134.6033	2.08	0	24	0.12	1	U	K.TQVAGGQLSPK.G
✓ 1593	638.8448	1275.6751	1275.6744	0.57	0	58	4.7e-05	1	U	K.TAVLDAIDLAK.K + Oxidation (M)
✓ 1902	704.3607	1406.7069	1406.7041	1.95	0	44	0.00094	1	U	R.VINLNDNFTFEK.G
✓ 2224	879.9641	1757.9135	1757.9047	5.02	0	71	2.2e-06	1	U	R.VSVLIQQDTSDPEK.V

Proteins matching the same set of peptides:
[sp|P46061|RAGP1_MOUSE](#) Mass: 64090 Score: 230 Matches: 5(4) Sequences: 5(4)
Ran GTPase-activating protein 1 OS=Mus musculus GN=Rangap1

Sumoylated RanGap1 identified from gel slice with MW range from 80-100 kD

[tr|Q6NZB5|Q6NZB5_MOUSE](#) Mass: 64005 Score: 30 Matches: 1(1) Sequences: 1(1) emPAI: 0.05
Rangap1 protein OS=Mus musculus GN=Rangap1
 Check to include this hit in error tolerant search or archive report

Query	Observed	Mr(expt)	Mr(calc)	ppm	Miss	Score	Expect	Rank	Unique	Peptide
✓ 1231	704.3654	1406.7162	1406.7041	8.55	0	30	0.028	1	U	R.VINLNDNFTFEK.G

Proteins matching the same set of peptides:
[tr|E9Q2J7|E9Q2J7_MOUSE](#) Mass: 43303 Score: 30 Matches: 1(1) Sequences: 1(1)
Uncharacterized protein OS=Mus musculus GN=Rangap1
[sp|P46061|RAGP1_MOUSE](#) Mass: 64090 Score: 30 Matches: 1(1) Sequences: 1(1)
Ran GTPase-activating protein 1 OS=Mus musculus GN=Rangap1

Figure S2

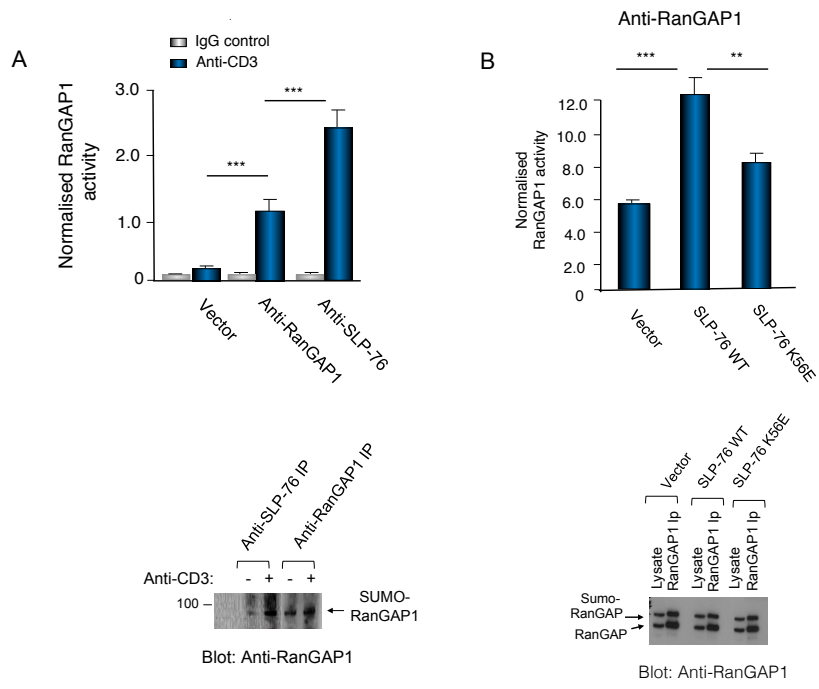
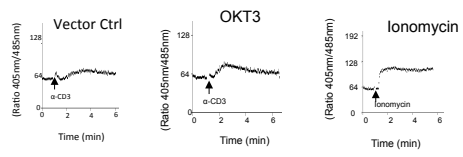


Figure S3

A



B

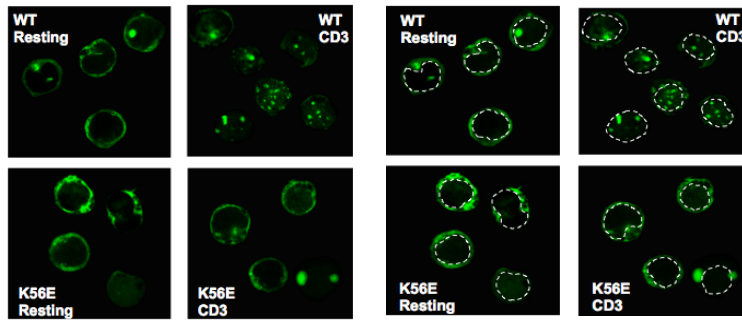
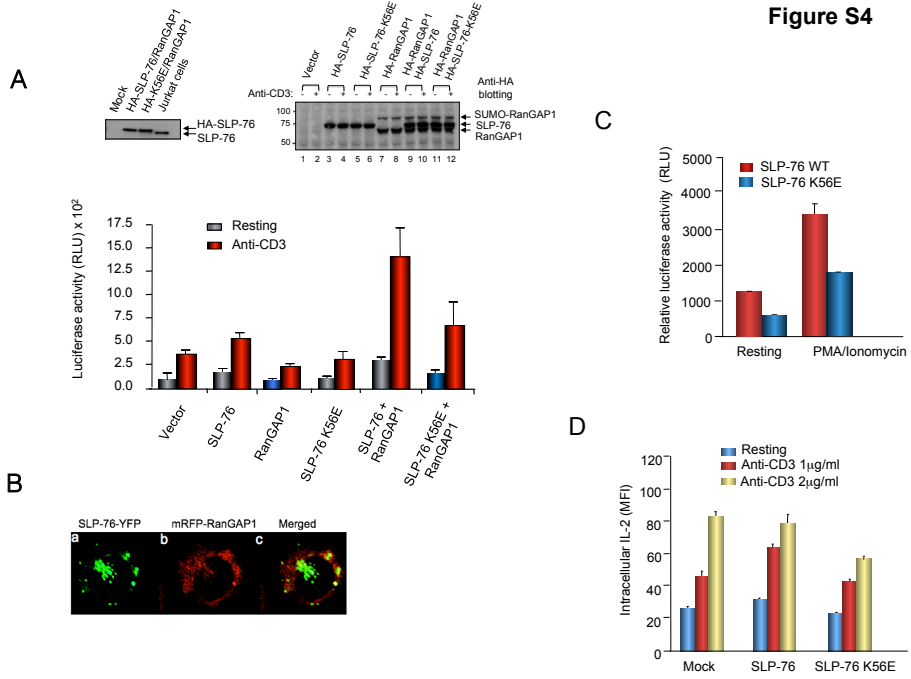


Figure S4



SUPPLEMENTAL FIGURE LEGENDS

Figure S1: (A) SLP-76 binds to RanGAP1 and not to RanBP2, Related to Figure

1. Upper panel: SLP-76 binds to RanGAP1 co-expressed in 293T cells. 293T cells were transfected with control vector (lane 1) or SLP-76 WT (lane 2), subjected to immune precipitation with anti-RanGap1 and blotted for SLP-76 or RanGAP1. Anti-RanGAP1 co-precipitated SLP-76 (lane 2). Lower panel: SLP-76 does not bind to RanBP2 co-expressed in 293T cells. 293T cell lysates (left) and anti-RanBP2 immune precipitates (right) from mock control vector (lanes 1, 3) or GFP-RanBP2/HA-SLP-76 (lanes 2, 4). Transfectants were then blotted with anti-SLP-76 or anti-GFP. Anti-RanBP2 precipitated itself (lane 4-band lower than slight higher non-specific band in mock control) but not SLP-76 (lane 4) from GFP-RanBP2/HA-SLP-76 WT transfected cells. (B) SLP-76 binds to RanGAP1, but not to NFATc1. Jurkat cells were ligated with anti-CD3 for 10min (lanes 2,4,6) followed by immune precipitation using mIgG (lanes 1,2); anti-NFATc1 (lanes 3,4); anti-SLP-76 (lanes 5,6). While anti-CD3 increased RanGAP-1 co-precipitated by anti-SLP-76 (lane 6 vs. 5), anti-NFATc1 failed to precipitate SLP-76 (lanes 3,4) and vice versa (lane 5,6). Anti- NFATc1 also failed to co-precipitate RanGAP1 (lanes 3,4). (C) RanGAP1 in anti-SLP76 precipitates confirmed by MALDI-MS/MS spectrometry. Upper left panel: Colloidal Blue staining of proteins precipitated by anti-SLP-76 or isotope mouse IgG control from mouse T8.1 cells. Upper right panel: Blotting of anti-SLP-76 precipitates from quantitative isolation showing RanGAP1 and GADs. Middle box: List of SLP-76 interacting proteins identified in mouse T8.1 cells by mass spectrometry. Lower Box: List of RanGAP1 peptides identified in anti-SLP76 immune precipitates via LC-MS/MS analysis.

Figure S2: SLP-76 binding to RanGAP1 regulates exchange activity, Related to

Figure 2. (A) Higher RanGAP1 exchange activity in anti-SLP-76 compared to anti-RanGAP1 precipitates. T8.1 cells were either incubated with IgG control or anti-CD3

for 5min followed by precipitation from lysates with mouse IgG, anti-SLP-76 or anti-RanGAP1. GTPase exchange activity involving Ran GTP hydrolysis was measured as in *Experimental Procedures*. Exchange activity was normalized relative to the amount of RanGAP1 precipitated by anti-SLP-76 or anti-RanGAP1 as detected by anti-RanGAP1 blotting. Background levels of activity associated with cells treated with the IgG control were then subtracted from values obtained from cells ligated with anti-CD3. The normalised activity in the anti-SLP-76 precipitates was then subtracted from the normalized activity in the anti-RanGAP1 precipitates to obtain the activity values for SLP-76 free RanGAP1. Upper panel: histogram showing normalized RanGAP1 exchange values. Lower panel: Western blotting showed RanGAP1 protein precipitated by anti-SLP-76 and anti-RanGAP1. Statistical significance by mean +/- SEM; *p<0.05, ; **p<0.01; ***p<0.001. (B) Lower exchange activity in anti-RanGAP1 precipitates from J14 cells expressing K56E versus wild-type SLP-76. SLP-76 deficient J14 T cells were transfected with SR α empty vector, HA tagged SLP-76 WT or the K56E mutant. 24 hours later, cells were stimulated with anti-CD3 for 10 minutes followed by cell lysis and precipitation with anti-RanGAP1. A measurement of *in vitro* RanGAP1 activity assay was the performed as in *Experimental Procedures*. Exchange activity was normalized relative to the amount of RanGAP1 precipitated by anti-RanGAP1. Upper panel: histogram showing normalized RanGAP1 exchange values. Lower panel: Western blotting showed RanGAP1 protein precipitated by anti-RanGAP1. Statistical significance by mean +/- SEM; *p<0.05, ; **p<0.01; ***p<0.001.

Figure S3. Calcium influx and NFAT nuclear entry, Related to Figure 3. (A)

Calcium influx is similar in J14 cells expressing SLP-76 WT vs K56E mutant. SLP-76 deficient J14 cells transfected with vector control vs. pcDNA-SLP-76 WT or K56E mutant were subjected to calcium influx measurement with Indo-1. Calcium influx was monitored by flow cytometry at excitation wavelengths of 480 and 405 nm using

a Becton Dickinson CyAn cytometer. (B) Delineation of the nucleus vs. cytoplasm. Delineation of the nucleus vs. cytoplasm (dotted lines) showing that anti-CD3 induced NF-ATc1 nuclear translocation is impaired in J14 cells expressing K56E. J14 cells were co-transfected with NF-ATc1-GFP together with either HA-SLP-76 wild type or HA-SLP-76 K56E followed by anti-CD3 (2 μ g/ml) ligation for 15 minutes, fixation with BD Cytofix/Cytoperm and staining with anti-HA (Alexa Fluor 633). Left panels show examples of NF-ATc1-GFP localization in transfected cells; right panels show examples of the cells with lines that delineate NF-ATc1-GFP localization in the cytoplasm and nucleus (i.e. based on DAPI staining).

Figure S4. SLP-76 and RanGAP1 synergize while binding is needed for optimal PMA/ionomycin induced NFAT activation, Related to Figure 4. (A) SLP-76 and RanGAP1 synergize to increase anti-CD3 induced NFAT1c driven transcription, and this effect is impaired by the K56E mutant. Jurkat J14 cells were co-transfected with the NFAT driven luciferase reporter together with SR α 2 based expression constructs encoding empty vector as a control, HA-RanGAP1, HA-SLP-76 WT, HA-SLP-76-K56E, HA-SLP-76-WT/HA-RanGAP1 and HA-SLP-76 K56E/HA-RanGAP1. Cells were stimulated with 0.1ug/ml anti-CD3 followed by a measure of luciferase activity as described above. Left panel: histogram showing SLP-76 and RanGAP1 synergy and its reduction by K56E mutation. Upper inset: immune blot showing similar levels of transfected HA-tagged SLP-76 versus K56E expression in J14 cells relative to normal endogenous SLP-76 in parental Jurkat cells. Right panel: immune blot showing protein levels in lysates from transfected J14 cells for HA-SLP-76, HA-SLP-76 K56E and HA-RanGAP1. Data are means of +/- SD from a representative experiment (n=4). (B) Immunofluorescence staining pattern of SLP-76-YFP and mRFP-RanGAP1 in transfected T-cells. Jurkat T-cells were co-transfected with SLP-76-YFP and mRFP-RanGAP1 followed by 24 hours post-transfection, stimulated with

anti-CD3 (2 μ g/ml) for 15 mins, followed by incubation with BD Cytofix/Cytoperm fixation solution. (a): SLP-76-YFP; (b): mRFP-RanGAP1; (c): merged panel. Both SLP-76-YFP and mRFP-RanGAP1 are localized to the cytoplasm. The intense insertional labeling corresponds to the Golgi region between lobes of the nucleus. (C) RanGAP1 binding to SLP-76 is needed for optimal PMA/ionomycin induced NFAT activation. J14 cells were co-transfected with SLP-76 (wild-type) or the K56E mutant plus a luciferase reporter construct carrying the NF- κ B sequences from the interleukin 2 promoter. Cells were stimulated with PMA/ionomycin followed by harvesting of the cells and measurement of luciferase activity some 6 hours later. Data are means of \pm SD from a representative experiment (n=3). (D) SLP-76 K56E inhibits anti-CD3 induced IL-2 production as measured by intracellular staining. Pre-activated and rested primary mouse T-cells were transfected with mock (SR α vector), SLP-76 WT or SLP-76 K65E and left either untreated or activated with anti-CD3 (1 and 2 μ g/ml) for 24 hours prior to intracellular staining with anti-IL-2. Data are means of \pm SD from a representative experiment (n=4).

Movie S1: Real time movie of micro cluster formation at the interface of anti-CD3 (OKT3)-coated coverslips with SLP-76 WT-EYFP-transfected J14 (left panel) and SLP-76 K56E-EYFP-transfected J14 T cells (right panel). Related to Figure 3.

EXTENDED EXPERIMENTAL PROCEDURES

Cell culture and reagents

Jurkat T-cells, were obtained from the ATCC, while the SLP-76 deficient Jurkat J14 T- cells were a kind gift from A. Weiss, UCSF. Mouse hybridoma T8.1 is a murine T cell hybridoma expressing human CD4 and a chimeric human–mouse TCR specific for a tetanus toxin peptide (830–843) restricted by HLA-DRB1*1102 or HLA-DRB1*1301 (Blank et al., 1993)(a gift from O. Acuto, Oxford). DC27.10 cells

were originally derived from the mouse cell line DO-11.10 and is an L3T4 positive, L α 2,3-negative T cell hybridoma (Marrack et al., 1983) as has previously described in the lab (Liu et al., 2010; Raab et al., 1999; Schneider et al., 2008). Antibodies included anti-human CD3 (OKT3), hamster anti-mouse CD3 2C11 (ATCC), anti-SLP-76 (BioXcell, West Lebanon, NH), anti-RanGAP1 (Santa Cruz Biotechnology, Santa Cruz, CA, USA), Mab414 (Covance), anti-SUMO1 (a gift from R. Hay, Dundee, UK), anti-Carma1 (Cell Signaling, Danvers, MA), anti-HA (Covance), anti-Lck, anti-ADAP, anti-SKAP1 and anti-GADS (Upstate Biotechnology, Lake Placid, NY), anti-NF-ATc1 (Santa Cruz Biotechnology, Santa Cruz, CA, USA), anti-RanBP2 (Thermo scientific); Monoclonal antibody against nuclear pore complex Mab414 (Covance), anti-actin (Sigma-Aldrich, Inc., St. Louis, OM, USA). CFSE (carboxyfluorescein diacetate succinimidyl ester) was purchased from Sigma (Poole, UK)

Expression vectors and plasmids

SLP-76-HA was constructed by sub-cloning SLP-76 cDNA into the *Xba*I /*Kpn*I sites of SR α 2 vector or into the *Xba*I /*Kpn*I sites of pCDNA3.1(-) vector with N-terminally 2XHA tags. RanGAPRanGAPHA tagged RanGAP1 was constructed by sub-cloning human RanGAP1 cDNA into the *Xba*I/*Kpn*I sites of SR α 2 vector. mRFP-RanGAP1 was constructed by sub-cloning human RanGAP1 cDNA into the *Bgl*II/*Hind*III sites of pMaxFp-red C1 vector (Amara). For SLP-76-YFP fusion construct, the human SLP-76 cDNA was amplified by PCR and was subcloned into the *Xho*I/*Bam*HI sites of pEYFP-N1 vector (Clontech). The constructs coding for K56E SLP-76 mutant fused to HA and EYFP were generated by point mutations of lysine to glutamic acid using a site-directed QuikChange mutagenesis kit (Stratagene) with primers: 5'- gacatccaggagttccccaagctccgggtg -3' and 5'- caccggagcttggggaactcctggatgctc-3'. The pcDNA based NFATc1 with C-terminally

GFP fusion construct was a kind gift from M. Purbhoo, London. The GFP-RelA/p65 construct was purchased from addgene (Cambridge, MA, USA).

Transfection and stimulation

Jurkat and J14 T -cells were transfected by microporation (Digital Bio Technology), using a single pulse of 30 ms at 1410 V, and mouse DC27.10 cells with 2 pluses of 20 ms at 1400 V. To activate Jurkat cells, 5×10^6 cells were incubated with pre-warmed RPMI 1640 media supplemented with 2% FCS with either 2 $\mu\text{g}/\text{ml}$ rabbit anti-mouse antibody or 2-5 $\mu\text{g}/\text{ml}$ of 145-2C11 (anti-CD3e) plus 2 $\mu\text{g}/\text{ml}$ rabbit anti-mouse antibody at 37°C for varying lengths of time. Peripheral blood human lymphocytes were isolated from buffy-coats by density gradient centrifugation and stimulated using the same regime. Human primary T -cells were transfected using a single pulse of 20 ms at 2259 V. To activate DC27.10 T cells, cells in in log growth phase were pelleted by centrifugation (1500 rpm for 5 mins) and suspended in serum free RPMI medium. Cells were then either incubated with an Ig isotope (2 $\mu\text{g}/\text{ml}$), or stimulated with 2C11(2 $\mu\text{g}/\text{ml}$) at 37°C for various times. Primary naïve mouse cells were transfected with various vectors using the Amaxa Nucleofector Kit (Lonza, Germany) according to the manufacturer's instructions and stimulated using the same regime as outlined for DC27.10 cells.

RanGAP1 GAP activity assays

The *in vitro* RanGAP1 GAP activity was measured by both radioactive and non radioactive assays. Isotype labelling is shown in Figs 2B and Fig. S2A, while the non-radioactive protocol was used in Figure S2B. For radioactive labelling, 2.5 μg of human recombinant Ran (Sigma-Aldrich) was loaded with either cold GTP (15 mM) or [γ - ^{32}P] GTP (15 Ci/mm, PerkinElmer) in the presence of loading buffer (10 mM EDTA, 2 mM ATP, 4 mM DTT, and 50 mM HEPES, pH 7.4) in 150 μl . Loading mixture was incubated at room temperature for 30min, then diluted 10-fold into buffer

(5 mM MgCl₂, 1 mM DTT, 0.1 mg/ml BSA, 0.005% Tween 20, and 50 mM HEPES, pH 7.4). Unbound GTP was removed on a NAP-5 column (GE Healthcare) and eluted with 1 mL GAP buffer (20 mM Tris-HCl pH 8.0, 50 mM NaCl, 5 mM MgCl₂, 0.05% BSA). RanGAP activity, which measures RanGTP hydrolysis, was then quantified using either a Phos-Free Phosphate Assay Kit (Cytoskeleton Inc., Denver, CO) according to manufacturer's protocol or isotope labelled *in vitro* RanGAP1 GAP activity assay as described (Bischoff et al., 1994). For a measurement of activity in precipitates, 40 µl of 60 nM Ran [γ ³²P] GTP (pre-loaded *in vitro*) was added to a volume of 10 µl of precipitate and incubated at 37°C. The GTPase reaction was stopped by addition of 1 ml of charcoal suspension [7% charcoal/10% ethanol/0.1 M HCl/10 mM KH₂PO₄]. After centrifugation at 10,000xg, the release of [γ ³²P] phosphate was determined in a liquid scintillation counter. Values associated with protein A beads in the absence of antibody was subtracted from values associated with anti-SLP-76 or RanGAP1 precipitates.

In the non radioactive assay, the release of free phosphate was measured as an increased in absorbance at 650 nm. RanGAP activity, which measures RanGTP hydrolysis, was then quantified using either a Phos-Free Phosphate Assay Kit (Cytoskeleton Inc., Denver, CO) according to manufacturer's protocol. Quantitation was based on the relative intensities of RanGAP1 in blots under conditions of non-saturated exposures. **p<0.01, ***p<0.001 vs SLP-76 WT. The average results were shown from three independent experiments.

Nuclear pore fraction isolation

Nuclear pore fractions were separated from cytoplasmic fractions of mouse hybridoma DC27.10 T -cells by using the Thermo NE-PER Nuclear and Cytoplasmic Extraction Kit (Fischer scientific). This involved a stepwise lysis of cells and centrifugal isolation of nuclear and cytoplasmic protein fractions. The nuclear extract

and nuclear envelope fraction containing nuclear pore complex were then extracted as previously described (Florens et al., 2008).

Immune precipitation and blotting

Immunoprecipitation and blotting were performed as previously described (Raab et al., 2011). Briefly, Jurkat, primary mouse or human T-cells were harvested and lysed with lysis buffer (20mM Tris-HCl, pH 8.0, 150mM NaCl, 1% (v/v) Triton X-100, 1 mM phenylmethylsulfonyl fluoride, 1 mM Na₃VO₄, 1mM NaF, 1mM leupeptin, 1mM pepstatin, and 1% aprotinin). Immunoprecipitation was carried out by incubation of the lysate with the antibody for 1 h at 4 °C, followed by incubation with 30 µl of protein A/G-agarose beads (50% w/v) for 1 h at 4 °C. For immune blotting, the immunoprecipitates were separated by SDS-PAGE and transferred onto nitrocellulose filters (Schleicher and Schuell). Filters were blocked with 5% (w/v) skimmed milk for 1 h in Tris-buffered saline pH 8.0 and then probed with the indicated primary antibody. Bound antibody was revealed with horseradish peroxidase conjugated corresponding secondary antibody using enhanced chemiluminescence (ECL, Amersham Biosciences).

Liquid chromatography tandem mass spectrometry (LC-MS/MS)

For LC-MS/MS (conducted by Cambridge Centre for Proteomics, Cambridge University), identification of SLP-76 associated proteins was made by peptide mass fingerprinting using trypsin digestion and a MALDI mass spectrometer. Anti-SLP-76 was precipitated from DC27.10 or T8.1 T-cells that had been stimulated for 24 hours with anti-CD3 (2C11) prior to detergent solubilisation. Gels were stained with colloidal on thin mini-gels to minimise the volume of gel and solutions were carefully filtered prior to use, wearing gloves at all times. After staining/destaining, image gels were washed in 10% (v/v) methanol to remove acid, gel bands were excised and subjected to the following treatment (30min per step, 20°C, in 200µl 100mM

ammonium bicarbonate/50% acetonitrile). This included reduction with 5mM tris(2-carboxyethyl)phosphine, alkylation by addition of iodoacetamide (25mM final concentration.) and digestion for 17h at 32°C in 25µl 100mM ammonium bicarbonate containing 5µg/ml modified trypsin (Promega). Peptides were then desalted using µC18 ZipTip (Millipore) and eluted to a MALDI target plate using 1.5µl alpha-cyano-4-hydroxycinnamic acid matrix (Sigma) in 50% acetonitrile/0.1% trifluoroacetic acid. Peptide masses were determined using a Maldi micro MX mass spectrometer (Waters) and analysed with Masslynx software. Database searches of the mass fingerprint data were performed using Mascot (<http://www.matrixscience.com>). For tandem ms/ms analysis, desalted peptides in were delivered to a ThermoFinnigan LCQ Classic ion-trap mass spectrometer using a static nanospray needle (Thermo Proxeon). Fragment ions were matched to possible sequence interpretations using MS-Product and/or MS-Tag (<http://prospector.ucsf.edu/>).

Immunofluorescence and Confocal Imaging

Cells were harvested, washed in PBS and fixed in Cytifix (BD Bioscience) for 30min at 4°C. Cells were then permeabilized in PBS containing 0.5% Saponin and 1% bovine serum albumin (BSA) for 90min with primary antibody for 1 h. Cells were then washed in PBS containing 0.1% Saponin and 1% BSA and incubated with fluorescently labeled secondary antibody for 1h. Incubation and washing for subsequent primary and secondary antibodies were repeated for double and triple-stained cells. After the final wash, cells were re-suspended in Vectashield mounting medium containing DAPI (4,6-diamidino-2-phenylindole; Vector Laboratories), mounted onto microscope slides, and sealed with nail varnish. Further live cell imaging on poly-L-lysine (Sigma) and anti-CD3 -treated cover slides (LabTek, Rochester, NY) was conducted as described (Bunnell et al., 2002; Bunnell et al., 2006; Liu et al., 2010; Purbhoo et al., 2010).

For staining of SLP-76 at the nuclear pore complex, mouse DC27.10 T-cells were either left untreated or stimulated with soluble anti-CD3 at 2 μ g/ml or the same concentration of hamster IgG as a control. Sequential immunofluorescence staining was then performed using primary antibodies, anti-SLP-76 (mouse IgG1) and anti-RanGAP1 (rabbit IgG) or MAb 414 (mouse IgG1). Cells were then washed in PBS at 4°C followed by staining using secondary antibodies Alexa Fluor 488 conjugated anti-mouse IgG, and Alexa Fluor 488 conjugated anti-rabbit IgG (Invitrogen) or anti-mouse IgG1 murine coupled Alexa Fluor 633. DAPI was used to stain the nuclei.

For imaging of NFATc1-EGFP, J14 cells were co-transfected with NF-ATc1-GFP together with either HA-SLP-76 WT or HA-SLP-76 K56E. 24 hours post-transfection, the cells were either mock-treated or stimulated with anti-CD3 (2 μ g/ml) for 15min, followed by incubation with BD Cytofix/Cytoperm fixation solution supplemented with DAPI, and staining with anti-HA (Alexa Fluor 633). The fluorescence intensity of NF-ATc1-GFP in the whole cell region (red dashed line circled) and in the nuclear region (the white dashed line circled) was quantified using the Image J program, from which the percentages of nuclear NF-ATc1-EGFP were calculated. Quantification of nuclear/total for NFATc1-EGFP was carried out for T-cells either expressing SLP-76 WT or K56E mutant with or without anti-CD3 stimulation.

Image acquisition was performed with a Zeiss LSM510 confocal microscope using a 63 Plan Apochromat/1.4- numerical-aperture oil objective lens. Lasers of 405-nm (DAPI)-, 488-nm (GFP and Alexa Fluor 488)-, 514-nm (EYFP), 594-nm (mRFP) and 633-nm (Alexa Fluor 647) wavelengths were used for fluorescence excitation. Images were processed with Leica confocal software (LCS; Leica Microsystems), Volocity (Improvision), and ImageJ (National Institutes of Health).

For imaging NF κ B nuclear translocation, J14 cells were co-transfected with GFP-RelA/p65 together with either HA-SLP-76 WT or HA-SLP76 K56E mutant. 24

hours post-transfection, cells were either left untreated or stimulated with anti-CD3 (2 μ g/ml) for 5 and 15 min. Cells were washed and fixed with 4% paraformaldehyde for 30 min. After permeabilization with 0.5% Saponin for 30 min, cells were washed and incubated with anti-HA antibody followed by Alexa Fluor 633 for 1 hour, respectively. After the final wash, cells were resuspended in Vectashield mounting medium containing DAPI (Vector Laboratories). Image acquisition was performed with a Zeiss LSM700 confocal microscope.

***In vivo* adoptive T-cell transfer assay**

For *in vivo* experiments, DO11.10 T-cells were isolated by using a mouse T-cell enrichment column kit (R&D, Abingdon, UK). DO11.10 T-cells were stimulated with anti-CD3 (2 μ g/ml) and anti-CD28 (5 μ g/ml) antibodies. The cells were pre-activated for 72 hours and then rested for 24 hours and were transfected with HA-SLP-76 or HA-SLP-76 K53E, labeled with CFSE (5 μ M). Cells were transfected with empty vector (mock), SLP-76 WT or SLP76 K56E using the Amaxa Nucleofector Kit (Lonza, Germany) (routinely gave up to 50-60% uptake efficiency). Transfected cells were labelled with CFSE and injected i.v. into the tail of Balb/c mice (4x10⁶ cells) followed by iv injection of 50 μ gOVA peptide 24 hours later. Proliferation of CFSE labelled T-cells was assessed 6 days after the OVA-peptide injections by FACS analysis.

Transmission electron microscopy (TEM)

Log growth phase DC27.10 T-cells with or without anti-CD3 stimulation (1 μ g/ml for 10min) were fixed by adding 1:1 double-strength fixative solution (8% PFA in 0.2 M phosphate buffer pH 7.4) to the culture medium for 5min followed by 2h in fresh 4% PFA in 0.2 M phosphate buffer pH 7.4 (Richardson and Leitch, 2007). Cells were then pelleted in 10% gelatin, infiltrated with 2.3 M sucrose and then frozen by

plunging into liquid nitrogen (Richardson and Leitch 2007). Frozen pellets were sectioned on a cryo-ultramicrotome (Leica, UC6 with FC6 cryo-attachment). Cryosections were thawed, rinsed in PBS with 1% glycine, incubated in PBS with 1% BSA, incubated with anti SLP76 antibody at a dilution of 1:50, rinsed in PBS and then incubated in secondary anti-mouse IgG antibody conjugated to 5 nm colloidal gold (Agar Scientific, UK). Alternatively anti-RanGAP was used at 1:400 to 1:2000 dilutions. Grids were then rinsed in PBS, transferred to 1% glutaraldehyde (Agar Scientific, UK) in PBS, washed in water and embedded in 2% methyl cellulose containing 0.4% uranyl acetate (Agar Scientific, UK). Images were taken on a Hitachi H7600 electron microscope. In order to measure the distances, since the cytoplasmic ring could not be directly visualised, first the distance from the central plane to the particle was measured, then the known distance (40 nm) from the central plane to the top of the cytoplasmic ring (Maimon et al., 2012) was subtracted to give the ring-label distance.

Measurement of intracellular calcium

SLP-76 deficient J14 cells transfected with pcDNA-SLP-76 WT or K56E mutant were subjected to calcium influx measurement (Parry et al., 2000). Briefly, cells were incubated at a density of 2×10^6 cells/ml in RPMI 1640, 1% FCS, and 5 μ M Indo-1 (Invitrogen) for 1 h before being washed twice in HBSS and re-suspended at 10^5 cells/ml in HBSS/0.2% FCS. After the addition of 2 μ g/ml anti-CD3 antibody or 1 μ g/ml ionomycin as a positive control, calcium influx was monitored by flow cytometry at excitation wavelengths of 480 and 405 nm using a Becton Dickinson CyAn cytometer. A total of 2 μ g/ml ionomycin (Sigma-Aldrich) served to elicit the maximum response while the relative concentration of intracellular free Ca^{2+} was measured as the median fluorescence ratio of Indo-1 bound/unbound (405/485 nm) over time. For statistical comparisons, the calcium response was normalized and expressed as the ratio of the maximum peak post-stimulation to baseline. Kinetic

plots were generated on ligated (Indo-1–labeled) cells using FlowJo software.

Promoter Reporter Assays and Intracellular FACs Staining

For the IL-2 NFAT luciferase reporter construct, Jurkat or J14 T-cells were transfected with an IL-2 promoter reporter vector (3 copies of NFAT binding sites and control vector (Promega, Madison, WI). 18 hours post-transfection, cells were either incubated with IgG isotype control or stimulated with various concentrations of anti-CD3 (0.1-1 μ g/ml anti-CD3) at 37 °C for 6 h and subsequently assayed for luciferase activity using a luminometer (MicroLumat, EG&G Berthold). Luciferase units of the experimental vector were normalized to the level of the control vector in each sample.

For the IL-2 NF- κ B luciferase (firefly) reporter plasmid, T-cells were transfected with the reporter plasmid together with Renilla luciferase plasmid (pRLTK, Promega) as an internal control to adjust for the transfection efficiency and background. Following 24 hours of expression, cells were ligated with anti-CD3 for six hours. Cells were then lysed in 100 μ l of lysis buffer of the dual luciferase assay kit (Promega). Light units were recorded on Luminometer (Berthold) from 10 μ l of sample in 100 μ l substrate solution as per the manufacturer's instructions. All the relative luciferase units (RLU) were derived by normalizing relative to internal Renilla values.

For intracellular FACs staining, primary murine T-cells were activated with anti-CD3 (5 μ g/ml) and anti-CD28 (5 μ g/ml) for 72 hours. Cells were then washed and after 24 hours transfected with Mock, SLP-76 WT and SLP-76-K56E mutant using the Amaxa Nucleofector Kit. 24 hours after transfection, cells were either left unstimulated or activated with plate-bound anti-CD3 (1 and 2 μ g/ml) for 48 hours. Brefeldin A was added 6 hours before fixation with 4% (v/v) paraformaldehyde. After

permeabilization with 0.5% (w/v) Saponin, the cells were stained with-phycoerythrin labeled anti-IL-2 and analyzed by FACS.

Bischoff, F.R., Klebe, C., Kretschmer, J., Wittinghofer, A., and Ponstingl, H. (1994). RanGAP1 induces GTPase activity of nuclear Ras-related Ran. *Proc Natl Acad Sci U S A* *91*, 2587-2591.

Blank, U., Boitel, B., Mege, D., Ermonval, M., and Acuto, O. (1993). Analysis of tetanus toxin peptide/DR recognition by human T cell receptors reconstituted into a murine T cell hybridoma. *Eur J Immunol* *23*, 3057-3065.

Bunnell, S.C., Hong, D.I., Kardon, J.R., Yamazaki, T., McGlade, C.J., Barr, V.A., and Samelson, L.E. (2002). T cell receptor ligation induces the formation of dynamically regulated signaling assemblies. *The Journal of cell biology* *158*, 1263-1275.

Bunnell, S.C., Singer, A.L., Hong, D.I., Jacque, B.H., Jordan, M.S., Seminario, M.C., Barr, V.A., Koretzky, G.A., and Samelson, L.E. (2006). Persistence of cooperatively stabilized signaling clusters drives T-cell activation. *Mol Cell Biol* *26*, 7155-7166.

Florens, L., Korfali, N., and Schirmer, E.C. (2008). Subcellular fractionation and proteomics of nuclear envelopes. *Methods Mol Biol* *432*, 117-137.

Liu, H., Purbhoo, M.A., Davis, D.M., and Rudd, C.E. (2010). SH2 domain containing leukocyte phosphoprotein of 76-kDa (SLP-76) feedback regulation of ZAP-70 microclustering. *Proc Natl Acad Sci U S A* *107*, 10166-10171.

Maimon, T., Elad, N., Dahan, I., and Medalia, O. (2012). The human nuclear pore complex as revealed by cryo-electron tomography. *Structure* *20*, 998-1006.

Marrack, P., Shimonkevitz, R., Hannum, C., Haskins, K., and Kappler, J. (1983). The major histocompatibility complex-restricted antigen receptor on T cells. IV. An antiidiotypic antibody predicts both antigen and I-specificity. *J Exp Med* *158*, 1635-1646.

Parry, C.M., Simas, J.P., Smith, V.P., Stewart, C.A., Minson, A.C., Efstathiou, S., and Alcami, A. (2000). A broad spectrum secreted chemokine binding protein encoded by a herpesvirus. *J Exp Med* *191*, 573-578.

Purbhoo, M.A., Liu, H., Oddos, S., Owen, D.M., Neil, M.A., Pagoon, S.V., French, P.M., Rudd, C.E., and Davis, D.M. (2010). Dynamics of subsynaptic vesicles and surface microclusters at the immunological synapse. *Science signaling* 3, ra36.

Raab, M., Kang, H., da Silva, A., Zhu, X., and Rudd, C.E. (1999). FYN-T-FYB-SLP-76 interactions define a T-cell receptor zeta/CD3-mediated tyrosine phosphorylation pathway that up-regulates interleukin 2 transcription in T-cells. *J Biol Chem* 274, 21170-21179.

Raab, M., Smith, X., Matthes, Y., Strebhardt, K., and Rudd, C.E. (2011). SKAP1 PH domain determines RAPL membrane localization and Rap1 complex formation for TCR activation of LFA-1. *J Biol Chem* 2011, 29663-70286.

Richardson, C.A., and Leitch, B. (2007). Identification of the neurotransmitters involved in modulation of transmitter release from the central terminals of the locust wing hinge stretch receptor. *Journal of Comparative Neurology* 502, 794-80.

Schneider, H., Smith, X., Liu, H., Bismuth, G., and Rudd, C.E. (2008). CTLA-4 disrupts ZAP70 microcluster formation with reduced T cell/APC dwell times and calcium mobilization. *Eur J Immunol* 38, 40-47.